

Full Length Article

Mechanisms of palmitate-induced lipotoxicity in osteocytes

Ahmed Al Saedi^{a,b}, Sandra Bermeo^c, Lilian Plotkin^d, Damian E. Myers^{a,b}, Gustavo Duque^{a,b,e,*}^a Australian Institute for Musculoskeletal Science (AIMSS), The University of Melbourne and Western Health, St. Albans, VIC, Australia^b Department of Medicine-Western Health, Melbourne Medical School, The University of Melbourne, St. Albans, VIC, Australia^c Facultad de Ciencias Básicas y Biomédicas, Universidad Simón Bolívar, Barranquilla, Colombia^d Department of Anatomy and Cell Biology, Indiana University School of Medicine in Indianapolis, IN, USA^e Sydney Medical School Nepean, The University of Sydney, Penrith, NSW, Australia

ARTICLE INFO

Keywords:

Apoptosis
Autophagy
Osteocytes
Fatty acids
Lipotoxicity
Palmitic acid

ABSTRACT

Background: Lipotoxicity is defined as cellular toxicity observed in the presence of an abnormal accumulation of fat and adipocyte-derived factors in non-fat tissues. Palmitic acid (PA), an abundant fatty acid in the bone marrow and particularly in osteoporotic bones, affects osteoblastogenesis and osteoblast function, decreasing their survival through induction of apoptosis and dysfunctional autophagy. In this study, we hypothesized that PA also has a lipotoxic effect on osteocytes *in vitro*.

Methods: Initially, we tested the effect of PA on osteocyte-derived factors DKK1, sclerostin and RANKL. Then, we tested whether PA affects survival and causes apoptosis in osteocytes. Subsequently, we investigated the effect of PA on autophagy by detecting the membrane component LC3-II (Western blot) and staining it and lysosomes with Lysotracker Red dye.

Results: PA decreases RANKL, DKK1 and sclerostin expression in osteocytes. In addition, we found that PA induces apoptosis and reduces osteocyte survival. PA also caused autophagy failure identified by a significant increase in LC3-II and a reduced number of autophagosomes/lysosomes in the cytoplasm.

Conclusion: In addition to the effects of PA on RANKL, DKK1 and sclerostin expression, which could have significant deleterious impact on bone cell coupling and bone turnover, PA also induced apoptosis and reduced autophagy in osteocytes. Considering that apoptosis and cell dysfunction are two common changes occurring in the osteocytes of osteoporotic bone, our findings suggest that PA could play a role in the pathogenesis of the disease. Suppression of these effects could bring new potential targets for therapeutic interventions in the future.

1. Introduction

Bone quality and quantity decreases with aging due to changes in the structural and material properties of bone [1], which is associated with increased skeletal fragility and fractures [2]. With aging, there is an increase in progenitor mesenchymal stem cell (MSC) differentiation to adipocytes over osteoblasts [3]. Increased expansion of adipocyte number in the bone marrow is associated with high levels of fatty acids within the bone marrow milieu, which has a variety of effects on bone cells including a toxic effect on osteoblasts, a phenomenon termed as lipotoxicity [4]. In bone, lipotoxicity involves the inhibition of osteoblast function and survival by adipocyte-secreted factors, predominantly palmitic acid (PA) [5,6]. In addition, adipocyte-secreted factors can reduce hematopoiesis and increase osteoclastogenesis by various mechanisms, which can alter bone turnover and lead to bone

loss [4,7].

Osteocytes, which derive from osteoblasts, are the most prevalent bone cells and reside within cavities called lacunae [8]. Osteocytes are terminally differentiated from osteoblasts and long cell projections from the osteocytes connect to the bone surface through these processes that travel through canaliculi. Specific surface markers are expressed on osteocytes during the different stages of their differentiation [9]. Osteocytes act as ‘sentinels’ that can regulate and modulate bone remodeling and also exhibit endocrine functions through the secretion of proteins that regulate bone formation [8]. Like osteoblasts, osteocytes express important cell regulatory molecules including membrane-bound receptor activator of nuclear factor kappa-B ligand (RANKL), Dickkopf WNT signalling pathway inhibitor1 (DKK1) and sclerostin [8]. High levels of apoptotic osteocytes and many compromised empty lacunae are observed in aging and in osteoporotic bone [10,11],

* Corresponding author at: Sunshine Hospital, 176 Furlong Road, St Albans, VIC 3021, Australia.

E-mail address: gustavo.duque@unimelb.edu.au (G. Duque).

URL: <http://www.aimss.org.au> (G. Duque).

<https://doi.org/10.1016/j.bone.2019.06.016>

Received 11 February 2019; Received in revised form 15 June 2019; Accepted 17 June 2019

Available online 18 June 2019

8756-3282/ © 2019 Elsevier Inc. All rights reserved.

suggesting that these processes are associated with changes in the bone microenvironment that affect osteocyte function and survival. Loss of osteocytes in bone is associated with acceleration of bone resorption [12,13], with viable osteocytes in the vicinity of apoptotic cells expressing a high RANKL/OPG ratio and releasing osteoclastogenic signals [14]. Additionally, with aging, the reduction in osteoblast numbers affects osteocyte formation leading to a decrease in osteocyte density and mineralization of the osteocyte lacunae [15].

Previously, we and others have reported the intrinsic mechanisms of PA-induced lipotoxicity in osteoblasts, an effect exerted through induction of dysregulated autophagy and apoptosis in human osteoblasts *in vitro* [5,6]. Therefore, given that PA-induced autophagy and apoptosis are also the most common mechanisms of lipotoxicity in other organs and tissues [16,17], and that autophagy and apoptosis are common features in age-related bone loss and osteoporosis [10], we hypothesized that PA could play an important role in the pathogenesis of osteocyte apoptosis and dysfunctional autophagy observed in aged and osteoporotic bone.

2. Materials and methods

2.1. Osteocytes

MLO-Y4-nGFP murine long bone osteocytes (kindly provided by Dr. Linda Bonewald, Indiana University, USA), were plated on 0.01% collagen-coated surfaces (Sigma, USA) and grown in α -MEM supplemented with 5% fetal bovine serum (FBS), 5% bovine calf serum (BCS), penicillin (100 U/ml) and streptomycin (100 μ g/ml). Cells were incubated at 37 °C under 5% CO₂. In order to maintain stable transfection in MLO-Y4-nGFP, 0.4 mg/ml G418 of antibiotic was added to the media.

2.2. Western blotting

Osteocytes were treated with PA (250 and 500 μ M), or vehicle alone, for 48 h. After various treatment conditions, osteocytes were lysed using lysis buffer (1% protease inhibitors) and centrifuged at 13000 g for 10 min to remove insoluble material. Before electrophoresis, protein concentrations were measured using the Pierce™ BCA Protein Assay Kit (Thermo Fisher Scientific, Scoresby, VIC, Australia) and samples were dissolved in SDS electrophoresis buffer. 10 μ g of protein per well were separated on SDS-polyacrylamide gels and subsequently electro transferred to a PVDF membrane for 50 min at 300 mA. After blocking with PBS containing 0.1% Tween 20 and 5% BSA, membranes were incubated overnight at 4 °C using primary antibodies against RANKL, Sclerostin (Santa Cruz, CA, USA, Cat:sc-130258), and DKK1 (Santa Cruz, CA, USA, Cat: sc-374574), or β -tubulin. The bound antibodies were detected with the appropriate corresponding secondary antibodies (1:10,000) conjugated with horseradish peroxidase. Blots were developed using enhanced chemiluminescence. For measuring autophagy, the same procedure was followed except a primary antibody anti-LC3 (Santa Cruz, CA, USA) was used instead. Quantification was performed using Image J software. Relative intensities of the bands were determined using tubulin as control.

2.3. Confocal microscopy

Cells were grown on collagen-coated coverslips in the absence or presence of PA (250 and 500 μ M). Cells were then fixed in 4% paraformaldehyde for 20 min and washed three times with PBS, permeabilized with 0.1% Triton X-100 in PBS for 10 min, washed and blocked with 5% BSA for 1 h. Anti-RANKL antibody (Abcam, 1:100, ab45039), was added and left overnight at 4 °C. Alexa555-conjugated anti-mouse antibody (Abcam, 1:1000 ab150110) was used for 45 min at room temperature as the secondary antibody. RANKL quantification was performed by calculating the fluorescence intensity of RANKL (red

channel) using ImageJ software. The red channel was chosen and then the image was threshold (converted to black-and-white) such that the red staining was represented by white pixels, then the histogram function of the software was used to obtain the total count. The same approach was used for the blue channel to count the number of nuclei in the field. Subsequently, the average staining level per cell was calculated. The same threshold setting and analysis was performed for all three different experiments using 6–8 images per condition.

To determine autophagy, LC3 (Sigma Aldrich, St. Louis, Missouri, USA), was used as the primary antibody for identifying autophagosomes. Alexa 488 conjugated donkey anti-rabbit (Sigma Aldrich, A-21206, St. Louis, Missouri, USA) was used as the secondary antibody. DAPI was added for 3 min, then cells were washed with PBS twice and Golden Pre-Long anti-fade (# P36930, Invitrogen) was added before analysis using a Leica SP5 confocal microscope. For identification of autophagolysosomes, Lyso-Tracker Red (LTR) dye (Life Technologies) (50 nM in media) was used for 30 min and cells were washed with PBS twice and antifade was added before analysis using a Leica SP5 confocal microscope. Control samples were incubated with secondary antibody alone. All images are at equal magnification and were processed and acquired identically (60 \times magnification using immersion oil).

2.4. Effect of PA on osteocyte viability

To determine the effect of PA on osteocyte viability, osteocytes were plated in 96-well plates at a density of 0.5×10^4 cells/cm². After an initial 24 h period in growth media (time 0), cells were treated with either PA (250 and 500 μ M) or vehicle alone. Cell viability was evaluated at timed intervals (24 and 48 h) by MTS assay (CellTiter 96® Aqueous One Solution Cell Proliferation Assay, Promega, Alexandria, NSW, Australia), according to the manufacturer's instructions. Viability was calculated as the percentage change compared with control. This experiment was repeated three times.

2.5. Flow cytometry

Osteocytes were treated with PA (250 and 500 μ M) and incubated in osteocyte media. After 48 h of incubation, apoptotic cells were quantified by Annexin V-PE staining. Briefly, osteocytes were harvested by centrifugation, washed with PBS and stained for 15 min at room temperature with Annexin V-PE and 7-ADD (BD Biosciences, Cat. No. 65875 \times , USA) in Annexin binding buffer, according to the manufacturer's instructions. The samples were then suspended in Annexin binding buffer and the level of fluorescence was determined using a BD FACS Verse flow cytometer with FlowJo software (BD Biosciences, USA). Annexin V-PE staining intensity from PA treated and untreated cells were compared to show the average fold increase in apoptotic cells. A dual histogram for Annexin V-PE vs 7-AAD was used to compare the apoptosis from PA-treated and untreated cells. Furthermore, to determine whether autophagy is affected by PA in osteocytes, cells were incubated with LTR dye (50 nM) for 3 min and the level of fluorescence was measured using a BD FACS Verse flow cytometer with Flow Jo software. Briefly, cells were washed in PBS buffer and trypsinized with lysis buffer. The cells were then washed with PBS and suspended in the presence of DNA viability dye, Propidium Iodide (PI) (Life Technologies, Cat. No. BMS500PI, CA, USA). LTR fluorescence intensity values from PA treated and untreated cells were compared to show the average fold increase in autophagy. A dual histogram was acquired to compare lysosomal fluorescence (representing LTR) with DNA viability dye (LTR+/PI+). Flow cytometry acquisition protocols were performed to collect approximately 10,000 events.

2.6. TUNEL assay

Cells were grown in collagen-coated plates and treated with PA (250 and 500 μ M) as previously described. Cells were then trypsinized and

fixed with 4% paraformaldehyde for 20 min at room temperature and then washed with PBS. TUNEL assay (Roche, Basel, Switzerland) for apoptosis was performed according to the manufacturer's instructions. The level of fluorescence was determined using a BD FACS Verse flow cytometer with Flow Jo software (BD Biosciences, USA).

2.7. Statistical analysis

All data are expressed as the mean of three replicate determinations, unless otherwise stated. Statistical analysis was performed by Student's *t*-test. *t*-tests were performed using a two-tailed distribution with two sample unequal variances. A probability value of $p < 0.05$ was considered statistically significant.

3. Results

3.1. PA reduces the expression of osteocyte-derived factors

Osteocytes are the most important producers of RANKL in bone [18]. Therefore, in this current study we investigated whether PA affects RANKL expression in osteocytes. We found a decrease in RANKL expression in osteocytes incubated with PA (Fig. 1A–C). The number of

RANKL-expressing cells was significantly reduced by the higher dose of PA (Fig. 1A and B). Western blot quantification showed a significant decrease in RANKL protein expression when the cells were incubated with 250 and 500 μM of PA ($p < 0.05$) (Fig. 1C and D). In addition, there was a significant decrease in DKK1 and sclerostin protein expression when cells were incubated with two concentrations of PA (250 and 500 μM) ($p < 0.05$) (Fig. 1E and F).

3.2. PA reduces survival and induces apoptosis in osteocytes

Initially, we determined cell viability in osteocytes treated with PA for 24 and 48 h (Fig. 2A). Treatment with 250 μM of PA resulted in 10% reduction of viability at 48 h as compared to control. In addition, treatment with 500 μM of PA resulted in 13% and 22% reduction of viability at 24 and 48 h, respectively, as compared to control ($p < 0.01$).

Apoptosis was quantified using two separate techniques: Annexin and TUNEL assays. Osteocytes were exposed to two different concentrations of PA (250 and 500 μM) or vehicle for 48 h. Fig. 2 (B and C) shows Annexin V positive (apoptotic cells quantified using flow cytometry). The total number of apoptotic cells comprises those in early and late apoptosis (Fig. 2C). While control cells showed 13.8% apoptosis

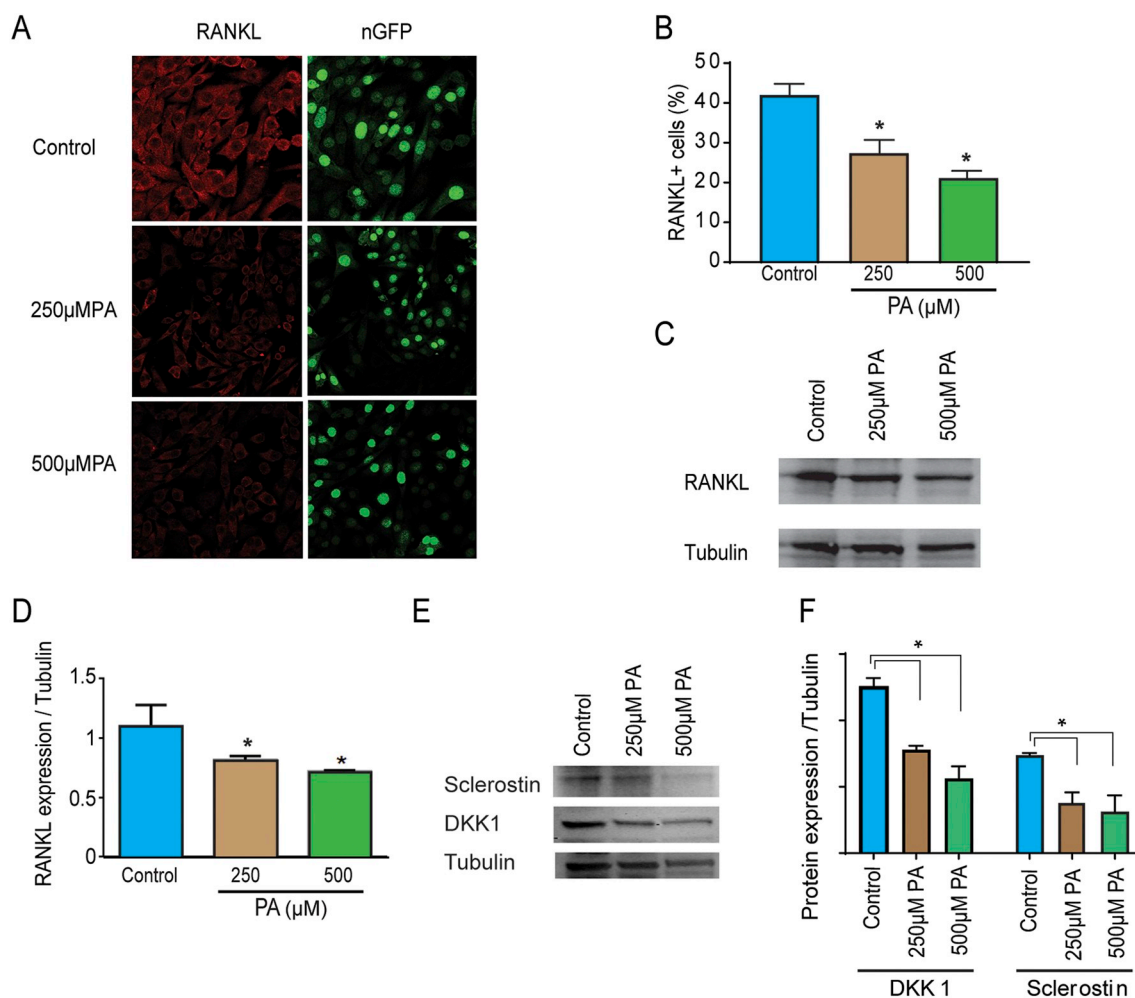


Fig. 1. PA reduces the expression of osteocyte-derived factors. (A) Osteocytes MLO-Y4-nGFP cells were treated with different concentrations of PA (250 and 500 μM) or control. Cells were fixed with 4% paraformaldehyde and stained with anti-RANKL. (B) Quantification of RANKL+ cells (%) from three different experiments using Image J software ($*p < 0.05$ vs control). (C) Osteocytes MLO-Y4-nGFP cells were treated with two different concentrations of PA (250 and 500 μM) or control. The figure illustrates the detection of RANKL by Western blot. Tubulin was used as a loading control. (D) Quantification of three different Western blot experiments using Image J software to analyze Western blot bands ($*p < 0.05$ vs control). (E) Osteocytes MLO-Y4-nGFP cells were treated with two different concentrations of PA (250 and 500 μM) or control, and Western blots were performed against Sclerostin and DKK1. Tubulin was used as a loading control. (F) Quantification of three different experiments using Image J software ($*p < 0.05$ vs control).

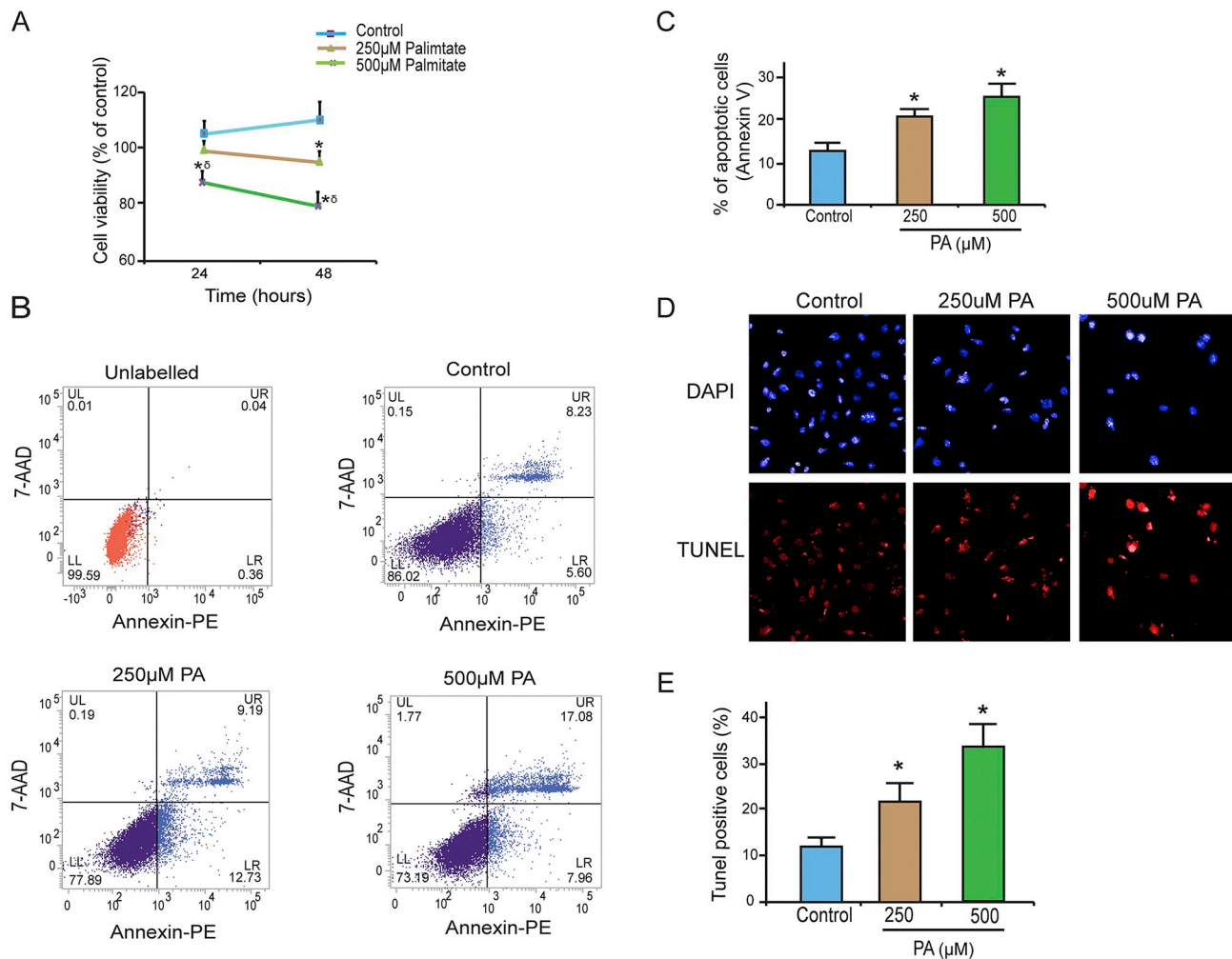


Fig. 2. PA reduces survival and induces apoptosis in osteocytes. **(A)** MLO-Y4 osteocytes were treated with PA for 24 h and 48 h and MTS assays were performed. Cell survival was significantly reduced under PA-treated conditions. Quantification of three different experiments (* $p < 0.05$ vs control; $op < 0.05$, 250 µM vs. 500 µM). **(B and C)** Flow cytometry analysis of apoptosis using a two-color (dual color fluorescence) histogram where the horizontal axis represents Annexin V-PE and the vertical axis represents 7-AAD. **(B)** Histograms shown are unlabeled cells, control cells, cells treated with 250 µM PA, and cells treated with 500 µM PA. **(C)** PA treatment induced a significantly higher number of Annexin V+ cells as compared with vehicle-treated cells (* $p < 0.01$ vs control). These results were confirmed by quantification of percentage of apoptotic cells by TUNEL assay **(D, E)** Osteocytes were treated with different concentrations of PA (250 and 500 µM) or vehicle for 48 h. Cells were fixed in 4% paraformaldehyde, permeabilized with Triton X-100, and a TUNEL assay was performed **(D)** and percentage of TUNEL positive cells was quantified by flow cytometry **(E)**. Data shown are mean \pm SD from three separate experiments (* $p < 0.01$ vs. control).

(early 5.6% and late 8.2%), cells cultured with 250 µM PA showed 21.9% apoptosis (early 6.7% and late 15.2%, $p < 0.01$), and cells cultured with 500 µM PA showed 25% apoptosis (early 8% and late 17%, $p < 0.01$). Quantification for apoptosis using TUNEL at 48 h (Fig. 2D and E) found 10% for the vehicle-treated cells vs. 24% and 36% for cells incubated with 250 µM and 500 µM PA respectively ($p < 0.01$).

3.3. PA decreases lysosome loading and recruitment in osteocytes

Osteocytes were incubated in the presence or absence of PA (250 and 500 µM) for 24 h and 48 h and analyzed by flow cytometry for expression of lysosomal loading by using a lysotracker dye. Flow cytometry analysis showed that PA caused significantly higher levels of lysosome loading compared to control cells (Fig. 3 A and B) ($p < 0.01$).

3.4. PA inhibits autophagy in osteocytes

We then investigated whether the increasing levels of lysosome loading in the cytoplasm induced by PA treatment were followed by

effective autophagy. In this case, osteocytes were cultured with three concentrations of PA (100, 250 and 500 µM). A lower dose of PA was used in these experiments to determine cell sensitivity to autophagy under a dose of PA that has not been toxic in previous studies [5,19]. Initially, expression of LC3 protein levels was measured as an indicator of autophagosomes in osteocytes. Western blotting quantification showed an increased expression of LC3-II protein when exposed to higher concentrations of PA but with no difference between the lower concentration of PA and the vehicle-treated controls (Fig. 4 A and B). These findings were confirmed as indicated by higher levels of LC3-II protein expression (punctate fluorescence staining using specific antibody) in the cytoplasm of PA-treated cells (Fig. 4C). To determine whether formation of autophagosomes and lysosomes recruitment was concomitant with efficient formation of autophagolysosomes, cells were incubated in the presence or absence of PA for 48 h with a lysotracker dye LTR and in combination with LC3 staining. Merged images for PA-treated cells showed lower colocalization of LC3-II and the lysotracker probe compared to osteocytes incubated with vehicle (control) (Fig. 4C and D).

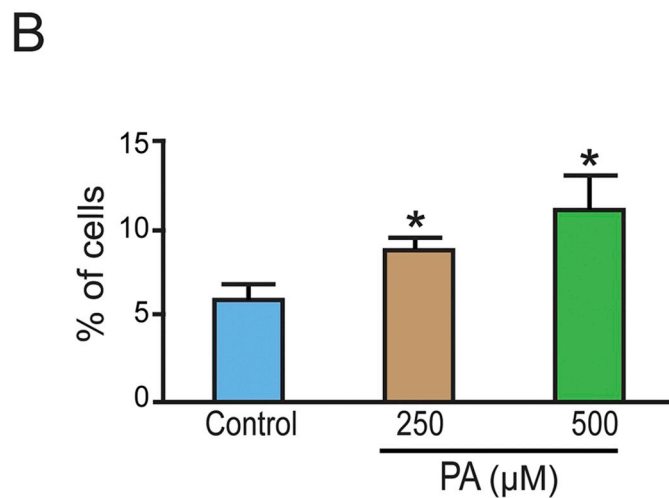
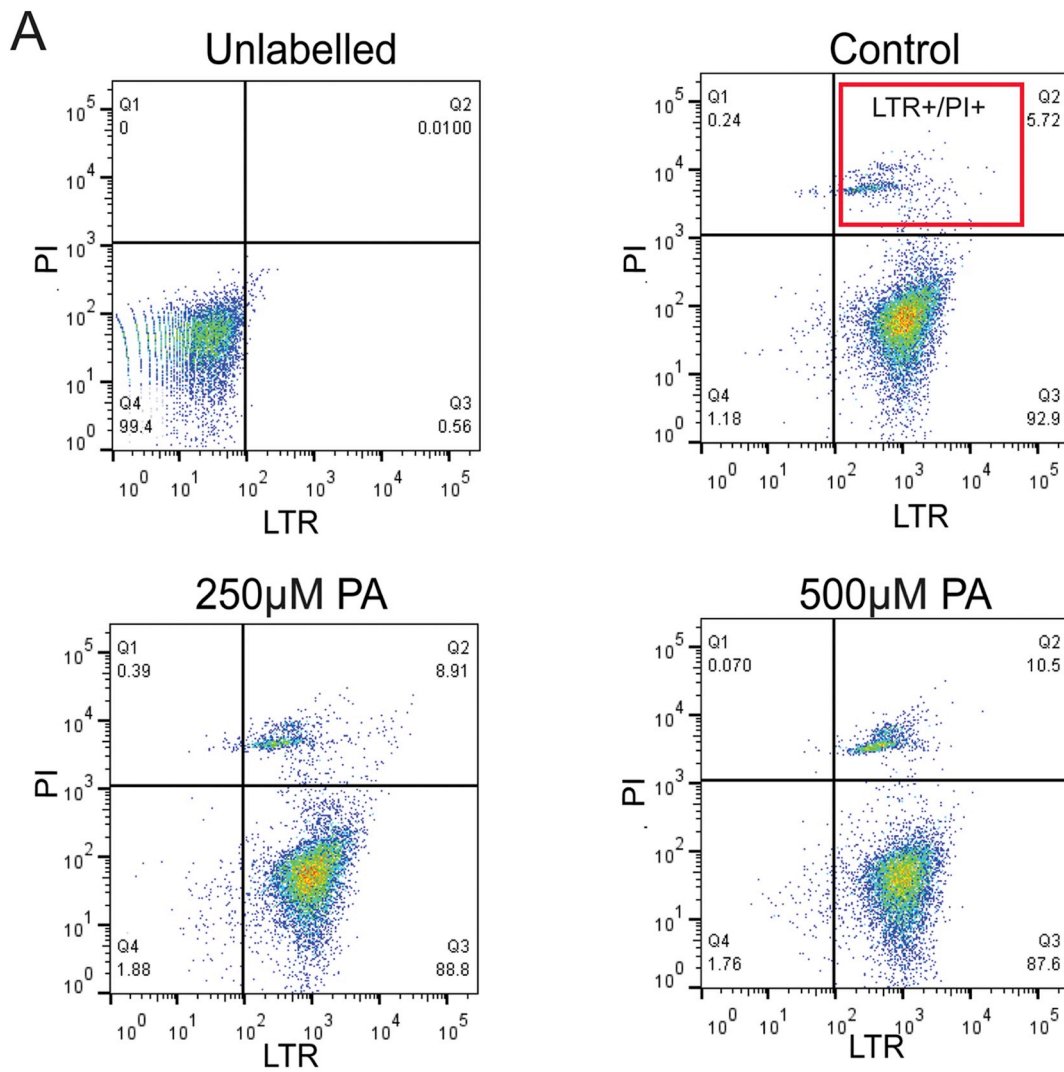


Fig. 3. PA treatment decreases lysosome content in osteocytes. **(A)** Cell were treated with PA for 48 h and analyzed by FACS analysis to measure excitation profiles for lyso-track red (LTR) dye. **(B)** PA treatment significantly increased lysosome content in osteocytes as compared with vehicle-treated cells. Data shown are mean \pm SD from three separate experiments. (* $p < 0.01$ vs. control). (For interpretation of the references to color in this figure legend, the reader is referred to the web version of this article.)

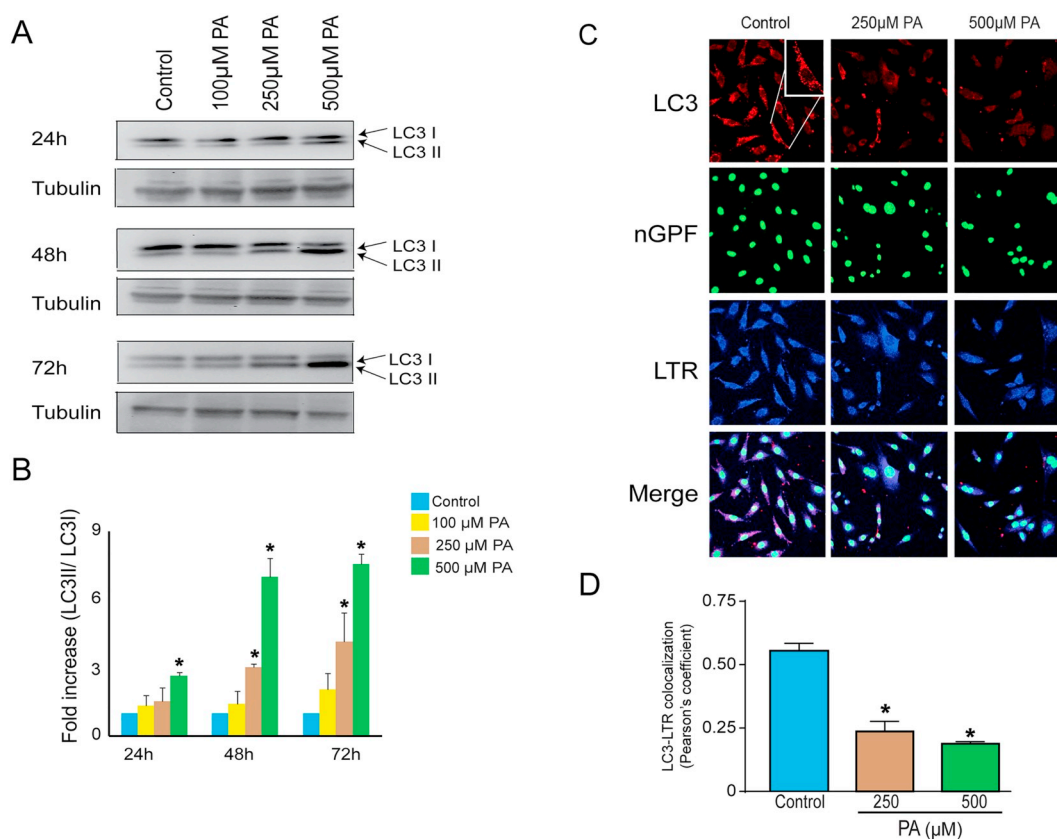


Fig. 4. Effect of PA on autophagy in osteocytes. **(A)** Osteocytes (MLO-Y4 cells) were treated with two different concentrations of PA (250 and 500 μM) or vehicle (control) and Western blot was performed against LC3 at 24, 48 and 72 Hrs. Tubulin was used as a loading control. **(B)** Quantification of three different Western blot experiments using Image J software. Treatment with PA increased the expression of the autophagy protein LC3-II in a concentration-dependent manner ($*p < 0.05$ vs control). **(C)** Images of osteocytes treated with two different concentrations of PA (250 and 500 μM) or control. Osteocytes were fixed with 4% paraformaldehyde and stained with anti-LC3, LTR and DAPI. Square in the first panel indicates punctate fluorescence staining using specific anti-LC3 antibody. All images are at equal magnification and were processed and acquired identically ($60\times$ oil) using a Leica confocal microscope and merged images were obtained using Image J software. **(D)** Quantification of three different experiments with LC3 expression using Image J software showing lower colocalization of LC3 and LTR indicative of dysfunctional autophagy ($*p < 0.01$ vs control).

4. Discussion

In this study we investigated the lipotoxic effect of PA on osteocytes. Since we have previously identified apoptosis and dysfunctional autophagy as the two main mechanisms involved in PA-induced lipotoxicity in osteoblasts *in vitro* [6], in this study we investigated whether the same mechanisms are involved in osteocyte lipotoxicity. Our results indicate that, as in osteoblasts, PA induces apoptosis and inhibits autophagy in osteocytes *in vitro*, which could partially explain the high levels of apoptosis and autophagy observed in osteocytes of aged and osteoporotic bone.

MLO-Y4 cells were utilized in this study as these cells model the properties of osteocytes and have proven to be useful for studying apoptosis and cell function related to mature osteocytes [12,20,21]. The presence of PA in the media affected the capacity of the osteocytes to express proteins that are essential for the regulation of bone turnover. Lower levels of RANKL could determine a low bone resorption and potential uncoupling. Furthermore, considering that DKK1 and sclerostin play crucial roles in bone remodeling, bone formation, and bone growth through their effects on osteoblast activity and survival [22,23], lower levels of these proteins induced by the presence of PA could significantly affect bone turnover. However, the implications of these findings on bone turnover could only be determined by future *in vivo* studies.

Apoptosis is an essential mechanism for bone health [24], however, increased osteocyte apoptosis could have a deleterious effect on bone as observed in aging mice where osteocyte apoptosis was accelerated by

loss of sex steroids [25]. In addition, osteocyte apoptosis was observed in high-dose corticosteroid treatment in human biopsies and mice samples [26]. Although osteocyte apoptosis could be induced by several factors, such as cytokines, hormones, pharmacological agents, and structural changes of bone [27], the mechanisms of age-related osteocyte apoptosis remain partially explored thus allowing us to hypothesize that this phenomenon could be associated with fatty acid-induced lipotoxicity, which could be the consequence of a fatty (and thus lipotoxic) bone marrow milieu. To test whether osteocytes are sensitive to toxic fatty acids, we used a similar approach to our previous work using PA, which is the most prevalent fatty acid within the human bone marrow milieu [28,29]. Our dosing was calculated as equivalent to the concentrations of PA in the human bone marrow [29], with a previously demonstrated lipotoxic effect on osteoblasts *in vitro* [5,6,19]. Overall, our results indicate that PA induces apoptosis in osteocytes *in vitro*, which could explain their lower rates of survival in the presence of PA in the media.

PA also induces lipotoxicity on osteoblasts *via* dysfunctional autophagy [6]. Autophagy is a lysosomal degradation process necessary for recycling cellular products. Autophagy is generally considered as a survival mechanism, which protects from apoptosis by removing damaged organelles, although in extreme stress it leads to cell death [30]. During the autophagy process, toxic cytoplasmic contents and damaged organelles trigger lysosomes recruitment, which then bind with phagosomes to form single membrane autophagosomes. The autophagic process requires many lysosomes to fuse with autophagosomes. It has been hypothesized that stimulation of autophagy would be anti-aging

whereas a reduction in autophagy would promote the aging process [31,32]. Indeed, healthy levels of autophagy are required to maintain an appropriate bone metabolism [33], however, as observed in age-related bone loss and osteoporosis, compromised autophagy could significantly affect bone turnover and bone mass [11,34].

PA-exposed osteocytes are expected to suffer from cellular stress. In an early stage, their response to PA could consist of lysosomes recruitment while attempting to remove the PA from the cytoplasm and protect the cells from lipotoxicity and cell death. If this mechanism of cell protection is affected by PA, it may eventually lead to cell death, as we have previously observed in human osteoblasts *in vitro* [6]. In our study, we identified that exposure of osteocytes to PA induced significantly higher levels of recruitment of lysosomes in the cytoplasm but without an effective formation of autophagolysosomes, thus suggesting that the presence of PA affected the autophagy process. These alterations in autophagy induced by PA treatment could then explain in part the higher level of apoptosis observed in the PA-treated cells.

In summary, we have found that, as in osteoblasts, PA induces lipotoxicity in osteocytes. Exposure of osteocytes to PA decreased their expression of osteocyte-derived factors, which are critical to normal bone turnover. In addition, PA induced lipotoxicity through apoptosis and inhibition of autophagy clearly mimicking the changes observed in osteocytes of aging and osteoporotic bone. However, the significance of these findings could only be determined using *in vivo* models. Most importantly, identification of a potential infiltration of marrow toxic fatty acids within the fluid flow through lacunae and canaliculi of bone, thus reaching the osteocytes and affecting their function and survival, will be a crucial component of future *in vivo* studies.

In conclusion, PA induces similar lipotoxic effects on osteoblasts and osteocytes *in vitro*. Although demonstration of this lipotoxic effect *in vivo* is still lacking, our results allow us to suggest that suppression of this lipotoxic effect *in vivo* could provide the basis to novel therapeutic approaches to osteoporosis in the future.

Acknowledgements

This study was supported by the Australian National Health and Medical Research Council (NHMRC 632767), the Nepean Medical Research Foundation, and the Australian Institute for Musculoskeletal Science (AIMSS).

References

- [1] E.A. Zimmermann, E. Schaible, H. Bale, H.D. Barth, S.Y. Tang, P. Reichert, B. Busse, T. Alliston, J.W. Ager 3rd, R.O. Ritchie, Age-related changes in the plasticity and toughness of human cortical bone at multiple length scales, *Proc. Natl. Acad. Sci. U. S. A.* 108 (35) (2011) 14416–14421.
- [2] D.P. Fyhrrie, B.A. Christiansen, Bone material properties and skeletal fragility, *Calcif. Tissue Int.* 97 (3) (2015) 213–228.
- [3] S. Muruganandan, R. Govindarajan, C.J. Sinal, Bone marrow adipose tissue and skeletal health, *Current Osteoporosis Reports* 16 (4) (2018) 434–442.
- [4] L. Singh, S. Tyagi, D. Myers, G. Duque, Good, bad, or ugly: the biological roles of bone marrow fat, *Current Osteoporosis Reports* 16 (2) (2018) 130–137.
- [5] K. Gunaratnam, C. Vidal, J.M. Gimble, G. Duque, Mechanisms of palmitate-induced lipotoxicity in human osteoblasts, *Endocrinology* 155 (1) (2014) 108–116.
- [6] K. Gunaratnam, C. Vidal, R. Boadle, C. Thekkedam, G. Duque, Mechanisms of palmitate-induced cell death in human osteoblasts, *Biology open* 2 (12) (2013) 1382–1389.
- [7] A.G. Veldhuis-Vlug, C.J. Rosen, Clinical implications of bone marrow adiposity, *J. Intern. Med.* 283 (2) (2018) 121–139.
- [8] L.F. Bonewald, The amazing osteocyte, *J. Bone Miner. Res. Off. J. Am. Soc. Bone Miner. Res.* 26 (2) (2011) 229–238.
- [9] L.F. Bonewald, Osteocytes as dynamic multifunctional cells, *Ann. N. Y. Acad. Sci.* 1116 (2007) 281–290.
- [10] R.S. Weinstein, S.C. Manolagas, Apoptosis and osteoporosis, *Am. J. Med.* 108 (2) (2000) 153–164.
- [11] S.C. Manolagas, A.M. Parfitt, What old means to bone, *Trends Endocrinol Metab* 21 (6) (2010) 369–374.
- [12] L.I. Plotkin, Apoptotic osteocytes and the control of targeted bone resorption, *Current osteoporosis reports* 12 (1) (2014) 121–126.
- [13] G. Gu, M. Mulari, Z. Peng, T.A. Hentunen, H.K. Vaananen, Death of osteocytes turns off the inhibition of osteoclasts and triggers local bone resorption, *Biochem. Biophys. Res. Commun.* 335 (4) (2005) 1095–1101.
- [14] O.D. Kennedy, M.B. Schaffler, The roles of osteocyte signaling in bone, *J. Am. Acad. Orthop. Surg.* 20 (10) (2012) 670–671.
- [15] H.M. Frost, Tetracycline-based histological analysis of bone remodeling, *Calcif. Tissue Res.* 3 (3) (1969) 211–237.
- [16] R.H. Unger, L. Orci, Lipopoptosis: its mechanism and its diseases, *Biochim. Biophys. Acta* 1585 (2–3) (2002) 202–212.
- [17] L. Martino, M. Masini, M. Novelli, P. Befly, M. Bugliani, L. Marselli, P. Masiello, P. Marchetti, V. De Tata, Palmitate activates autophagy in INS-1E beta-cells and in isolated rat and human pancreatic islets, *PLoS One* 7 (5) (2012) e36188.
- [18] T. Nakashima, M. Hayashi, T. Fukunaga, K. Kurata, M. Oh-Hora, J.Q. Feng, L.F. Bonewald, T. Kodama, A. Wutz, E.F. Wagner, J.M. Penninger, H. Takayanagi, Evidence for osteocyte regulation of bone homeostasis through RANKL expression, *Nat. Med.* 17 (10) (2011) 1231–1234.
- [19] A. Elbaz, X. Wu, D. Rivas, J.M. Gimble, G. Duque, Inhibition of fatty acid biosynthesis prevents adipocyte lipotoxicity on human osteoblasts *in vitro*, *J. Cell. Mol. Med.* 14 (4) (2010) 982–991.
- [20] H.M. Davis, R. Pacheco-Costa, E.G. Atkinson, L.R. Brun, A.R. Gortazar, J. Harris, M. Hiasa, S.A. Bolarinwa, T. Yoneda, M. Ivan, A. Bruzzaniti, T. Bellido, L.I. Plotkin, Disruption of the Cx43/miR21 pathway leads to osteocyte apoptosis and increased osteoclastogenesis with aging, *Aging Cell* 16 (3) (2017) 551–563.
- [21] L.F. Bonewald, Establishment and characterization of an osteocyte-like cell line, MLO-Y4, *J. Bone Miner. Metab.* 17 (1) (1999) 61–65.
- [22] M.K. Sutherland, J.C. Geoghegan, C. Yu, E. Turcott, J.E. Skonier, D.G. Winkler, J.A. Latham, Sclerostin promotes the apoptosis of human osteoblastic cells: a novel regulation of bone formation, *Bone* 35 (4) (2004) 828–835.
- [23] M.M. McDonald, A. Morse, A. Schindeler, K. Mikulec, L. Peacock, T. Cheng, J. Bobyn, L. Lee, P.A. Baldock, P.I. Croucher, P.P.L. Tam, D.G. Little, Homozygous Dkk1 knockout mice exhibit high bone mass phenotype due to increased bone formation, *Calcif. Tissue Int.* 102 (1) (2018) 105–116.
- [24] L.I. Plotkin, R.S. Weinstein, A.M. Parfitt, P.K. Roberson, S.C. Manolagas, T. Bellido, Prevention of osteocyte and osteoblast apoptosis by bisphosphonates and calcitonin, *J. Clin. Invest.* 104 (10) (1999) 1363–1374.
- [25] M. Almeida, L. Han, M. Martin-Millan, L.I. Plotkin, S.A. Stewart, P.K. Roberson, S. Kousteni, C.A. O'Brien, T. Bellido, A.M. Parfitt, R.S. Weinstein, R.L. Jilka, S.C. Manolagas, Skeletal involution by age-associated oxidative stress and its acceleration by loss of sex steroids, *J. Biol. Chem.* 282 (37) (2007) 27285–27297.
- [26] R.S. Weinstein, R.L. Jilka, A.M. Parfitt, S.C. Manolagas, Inhibition of osteoblastogenesis and promotion of apoptosis of osteoblasts and osteocytes by glucocorticoids. Potential mechanisms of their deleterious effects on bone, *J. Clin. Invest.* 102 (2) (1998) 274–282.
- [27] O. Verborgt, G.J. Gibson, M.B. Schaffler, Loss of osteocyte integrity in association with microdamage and bone remodeling after fatigue *in vivo*, *J. Bone Miner. Res. Off. J. Am. Soc. Bone Miner. Res.* 15 (1) (2000) 60–67.
- [28] R. Deshimaru, K. Ishitani, K. Makita, F. Horiguchi, S. Nozawa, Analysis of fatty acid composition in human bone marrow aspirates, *The Keio journal of medicine* 54 (3) (2005) 150–155.
- [29] J.F. Griffith, D.K. Yeung, A.T. Ahuja, C.W. Choy, W.Y. Mei, S.S. Lam, T.P. Lam, Z.Y. Chen, P.C. Leung, A study of bone marrow and subcutaneous fatty acid composition in subjects of varying bone mineral density, *Bone* 44 (6) (2009) 1092–1096.
- [30] Y. Tsujimoto, S. Shimizu, Another way to die: autophagic programmed cell death, *Cell Death Differ.* 12 (Suppl. 2) (2005) 1528–1534.
- [31] Y.S. Rajawat, Z. Hilioti, I. Bossis, Aging: central role for autophagy and the lysosomal degradative system, *Ageing Res. Rev.* 8 (3) (2009) 199–213.
- [32] F. Madeo, N. Tavernarakis, G. Kroemer, Can autophagy promote longevity? *Nat. Cell Biol.* 12 (9) (2010) 842–846.
- [33] V. Pierrefitte-Carle, S. Santucci-Darmanin, V. Breuil, O. Camuzard, G.F. Carle, Autophagy in bone: self-eating to stay in balance, *Ageing Res. Rev.* 24 (Pt B) (2015) 206–217.
- [34] M. Onal, M. Piemontese, J. Xiong, Y. Wang, L. Han, S. Ye, M. Komatsu, M. Selig, R.S. Weinstein, H. Zhao, R.L. Jilka, M. Almeida, S.C. Manolagas, C.A. O'Brien, Suppression of autophagy in osteocytes mimics skeletal aging, *J. Biol. Chem.* 288 (24) (2013) 17432–17440.